3D SIMULATION OF FLOW AROUND DIFFERENT TYPES OF GROYNE USING ANSYS FLUENT

A Dissertation submitted in partial fulfilment of the requirement for

the Award of the degree of

MASTER OF TECHNOLOGY

IN

HYDRAULICS & WATER RESOURCE ENGINEERING

BY

AASHISH MALIK
(ROLL NO. 2K14/HFE/01)

Under the Guidance of
Dr MUNENDRA KUMAR
Professor
Department of Civil Engineering

DELHI TECHNOLOGICAL UNIVERSITY
(FORMERLY DELHI COLLEGE OF ENGINEERING)
DELHI - 110042

July-2016

CANDIDATE'S DECLARATION

I do hereby certify that the work presented is the report entitled "3D Simulation of Flow Around Different Types of Groyne Using ANSYS FLUENT" in the partial fulfillment of the requirements for the award of the degree of "Master of Technology" in Hydraulics & Water Resource Engineering submitted in the Department of Civil Engineering, Delhi Technological University, is an authentic record of my own work carried out from January 2016 to July 2016 under the supervision of Dr. Munendra Kumar (Professor), Department of Civil Engineering.

I have not submitted the matter embodied in the report for the award of any other degree or diploma.

AASHISH MALIK

(2K14/HFE/01)

Date: 5/7/16

CERTIFICATE

This is to certify that above statement made by the candidate is correct to best of my knowledge.

Dr Munendra Kumar

(Professor) Department of Civil Engineering

Delhi Technological University

ACKNOWLEDGEMENT

I take this opportunity to express my profound gratitude and deep regards to Dr Munendra Kumar (Professor, Civil Engineering Department, DTU) for his exemplary guidance, monitoring and constant encouragement throughout the course of this project work. The blessing, help and guidance are given by him from time to time shall carry me a long way in life on which I am going to embark.

I would also like to thank Dr Nirendra Dev (Head of Department, Civil Engineering Department, DTU) for extending his support and guidance.

I would also like to thank Md. Mohsin (PhD scholar at IIT Delhi) for his support and guidance.

Professors and faculties of the Department of Civil Engineering, DTU, have always extended their full co-operation and help. They have been kind enough to give their opinions on the project matter; I am deeply obliged to them. They have been a source of encouragement and have continuously been supporting me with their knowledge base, during the study. Several of well-wishers extended their help to me directly or indirectly and we are grateful to all of them without whom it would have been impossible for me to carry on my work.

ABSTRACT

The objective of this project is to study flow pattern around a single spur-dike or groyne with free surface flow using a numerical model prepared in a software known as ANSYS FLUENT 16.0. Model is prepared to investigate the 3D turbulent flow field around a single straight (SD), two repelling type groyne 45^o and 60^o (RG-45 and RG60) and two different T-shape groynes: TF (groyne with full wing length) and TH (groyne with half wing length) under smooth flat-bed condition. The study shows intense effects on turbulent and mean flow characteristics of different shapes of the groyne, especially for the near-bed region. Amplification of near-bed velocity is due to contraction of the channel cross-section and as well as due to local effects of the groyne structure is higher in the case of SD and repelling groyne (RG-45 and RG-60) than that of T-shape groynes. Horseshoe vortex variation at the base of spur is more compact & strong rotational momentum in the case of RG-45 then others. Observed decreasing order of this compactness & rotational momentum is RG-45; RG-60; SD-90; TH & at last TF. Increased wing length in the case of full wing length T-shape groyne (TF) effects the flow structure at the upstream mini embayment. Dominantly horizontal circulation flow occurs in place of vertical, due to which horseshoe vortex disappears. So we can say that increased wing segment act as a scour countermeasure.

Keywords: Groyne/spur/dike; T-shape; Horseshoe vortex; Dynamic Shear layer

CONTENTS

Lists of Figures

List of Tables

CHAPTER-1

INTRODUCTION

The alluvial plain rivers are highly variable in the behaviour & unpredictable. During low flow condition it possesses no threat to existing structures, but during high flow condition it may cause unforeseen meanders, attack town and important structures, break through the embankment, outflank bridges. Therefore, each and every time when any hydraulic structure is built across an alluvial stream appropriate attempt in the form of river training works should be taken to maintain the river along the certain alignment with a predetermined cross-section. Such kind of works constructed to train the river is called river training works.

Purpose of river training works

The main objective of river training works includes to confine and guide the flow in a defined course & to regulate and control the river bed configuration for safe & effective movement of floods.

1.1 Various type of river training works

1. Groyne/ spurs
2. Guide bank
3. Artificial cutoff
4. Pitched island
5. Marginal embankments

1.2 Groynes/spurs

Groyne **(also known as spurs-dike)** are usually used in river engineering or bank support or navigation such as confine flow through bridge & in coastal engineering for beach protection works. Spur or groynes are transverse structures constructed across the flow to avoid bank erosion, outflanking of the existing structures and much more. These are provided with appropriate launching apron to prevent scouring under water & consequently results into the failure of the spur.

1.3 Important functions of spurs

1. Bank protection from the high-velocity current by maintaining the flow away from side bank and towards the centre position of the river.
2. By contracting the width of channel improving navigational depth.
3. Increases sediment deposition near river bank to improve the alignment of the channel.
4. Restoration of the river ecosystem.

1.4 Flow around a straight groyne (SD) includes

1. **Upstream of groyne** - flow separated from the channel side wall.
   Downstream of groyne – formation of quasi-periodic recirculating zone (Paik & Sotiropoulos 2005[1]).
2. Just upstream of the groyne, a stagnant vertical pressure gradient results in a strong down flow (Kwan 1988[2]).
3. Due to the interaction of down flow and the approach boundary layer formation of periodically oscillatory horseshoe vortex system (HSV) at the groyne base (Koken and Constantinescu 2009[3]).
4. Wake zone developed (reattachment zone and return flow).
5. A fully dynamic & turbulent dynamic detached shear length (DSL) in between the wall and main flow zone (Ehema and Muste 2004[4]; Koken and Constantinescu 2009[3]).
6. At groyne tip vortex shedding phenomena can be seen. (Paik and Sotiropoulos 2005[1]).

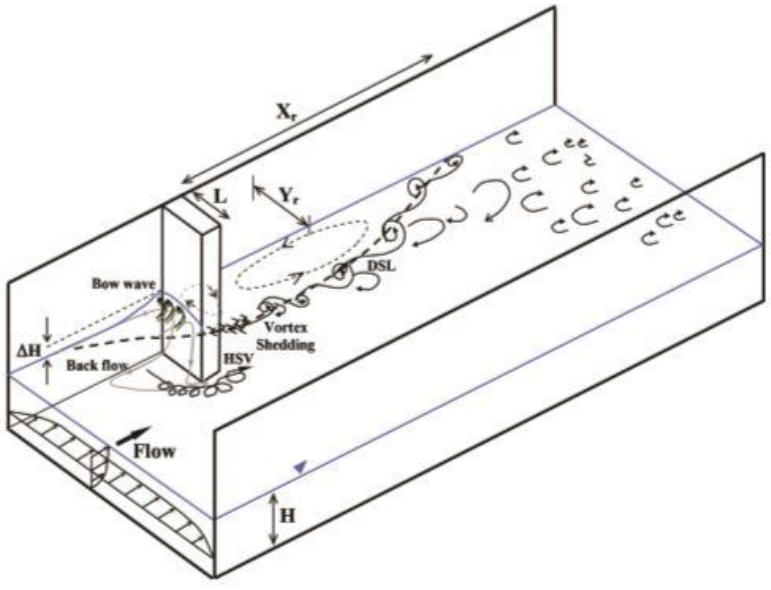

Fig. 1.1. Flow features around a single straight groyne.

1.5 Type of groynes

Groynes can be classified into four categories

1. **On the basis of method and material of construction**

   Permeable or Slotted and Impermeable

   Permeable groynes are kind of spurs which allow water to flow through them & are generally used in rivers with high sediment load, in case deposition of sediment is desired around spurs. Timber, bamboo or piles are generally used to construct them.

   Opposite to this impermeable groynes do not allow water to flow through them thus causing the water current to deflect. Generally used to protect the bank in the navigable channel where a greater depth of flow is required in the center of the stream. They can be made of gabion, rock or solid concrete structure.

Fig. 1.2. Impermeable Groyne

Fig. 1.3. Permeable groyne

2. **Submergence**

   Submerged, non-submerged and partially submerged

   Depending on the water depth. Impermeable groynes are generally designed to be non-submerged as they experience a high scour at their side walls when they are submerged. Permeable kind is designed as submerged because there is a smaller amount of local scour.

3. **Action of spur**

   Repelling, attracting, and deflecting groynes

Repelling groynes are spurs which make an acute angle with the upstream bank and repel the flow away from the bank. They are most commonly used for bank protection works.

Attracting groyne, which is pointed downstream or makes an obtuse angle with upstream bank & they attract the flow towards groyne downstream bank. They used when water is to attract towards the downstream bank of groyne depending on the condition.

Deflecting type of groynes is generally shorter groynes, which changes the direction of flow & deflect flow away from the bank. They are least popularly used.

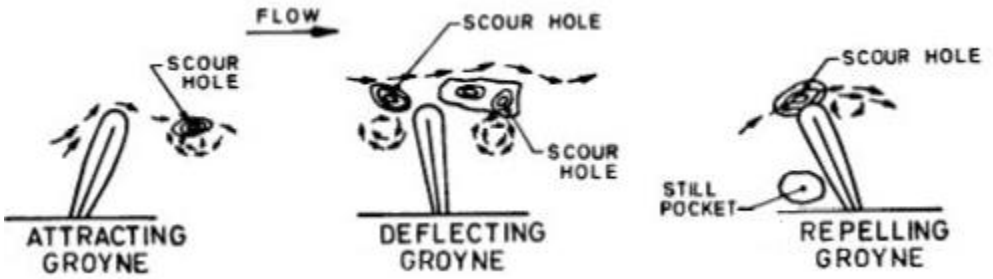

Fig. 1.4. Different groynes on the basis of action of spur

4. On the basis of shape

In the present day, many shapes of groynes are used depends on special conditions. Some these are T-head, L-head, hockey, straight round-headed, inverted hockey etc.

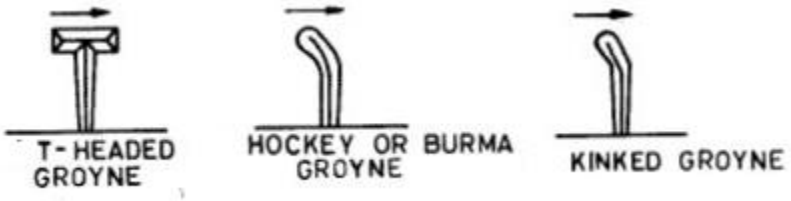

Fig. 1.5. Some of the different shapes of groynes

1.6 Design consideration

Some of the important design parameters

1. **Length of groyne:-**

   Groyne length depends on the purpose, location, spacing and economics of construction. Groyne length can be estimated by determining the width of the channel. Groyne length is limited up to 1/5 of the width of the channel by IS code 8408:1994 for planning and design of groyne in alluvial river guidelines. Also, length should not less than that to keep the scour hole, formed nearby nose, away from the bank.

2. **Spacing for series of groynes**

   Model studies are conducted to determine spacing for site-specific cases. Normally it is between 2 to 2.5 times its effective length of groynes in the case of a curve section. For a straight reach, if the discharge is kept nearly equal in two channels, the ratio of protected length to the length of the groyne is 3 times for wide channel than that of a narrow one.

   Longer spacing is normally permissible in straight reach than that of curved ones.

   Location of groynes also effects spacing. Larger spacing adopted for convex banks and similarly smaller spacing for the concave bank.

3. **Top level, top width and side slope**

   The top level depends on the type of groynes is to use namely non-submerged, partially submerged and submerged. The best type for specific channel size is decided after a model study.

   For non-submerged case, the top level of groyne should be above design flood level with some adequate freeboard. The freeboard generally adopted is 1mor 1.5m.

   For submerged case, the top level is kept similar to HFL. Top width of the groyne is kept 3 to 6m as per requirement.

   Side slope may be kept 2H:1V or #H:1V depends on the material used for construction.

1.7 Introduction to ANSYS FLUENT

In today's world computational fluid dynamics (CFD) is getting more & more popular. It is a mathematical tool in which there are vast possibilities to analyze various fields of engineering like fluid dynamics, electromagnetics, multiphysics, structural mechanics, hydrodynamics, and much more are using CFD. So, CFD base simulation is done by engineers of various fields is conducted on vast numbers of topics. The basic principal of applying CFD over a specified boundary condition is to determine fluid flow parameters in detail by solving a system of linear, non-linear governing equations over the region of interest. Simulation confides of combine modelling precision, numerical accuracy and post computational analysis.

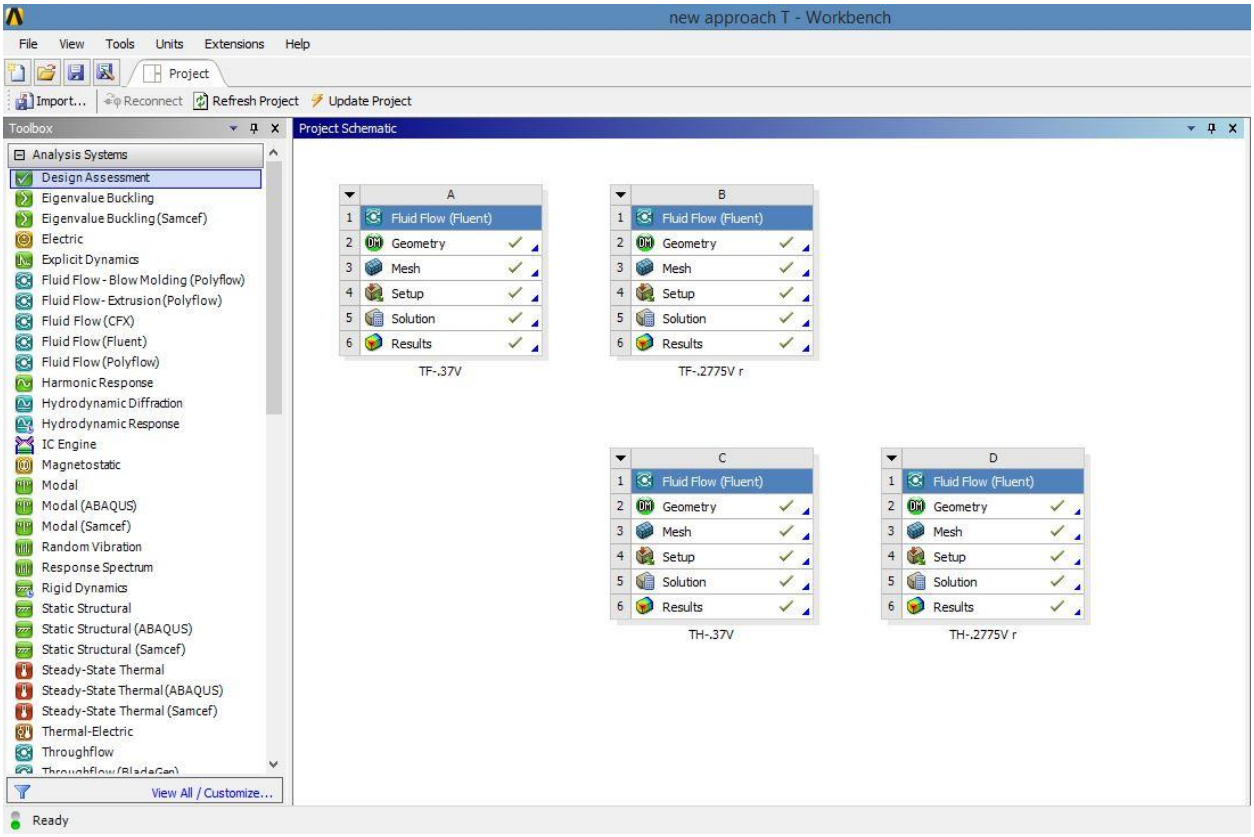

Fig. 1.6. ANSYS Workbench

Fluent is the computational fluid dynamics (CFD) solver for complex fluid flows. Ansys workbench contains Ansys Fluent as an integrated part of it. The fluent software gives a complete mesh adaptability, including the ability to solve flow problem flow problem using structured meshes than can be produced over complex geometries. Meshing types that supports are triangular,

cutoff, tetrahedral, hexahedral, pyramid, quadrilateral prism (wedge) and polyhedral. Dynamic refinement or coarsening of the mesh is also available in ANSYS based on user's choice. Ansys Fluent conveniently run for all physical models and flow conditions including transient or steady-state, compressible or incompressible flows, turbulent or laminar flow and Newtonian or non-Newtonian flows. Ansys Fluent consist of a various powerful solver for application: fully segregated pressure based solver coupled based solver, an explicit and implicit density based solver. The majority of open channel flows are turbulent in nature, so Ansys Fluent always pay a special priority in providing leading turbulent models to evaluate the effects of turbulence accurately.

Post processing tools of Ansys Fluent are used to produce meaningful graphics in the form contours, streamlines, and values at different points, excel sheet and also animations that make it user-friendly. So, fluid dynamics results can be shown easily. Streamlines, vector plots, pathlines, shaded & transparent surfaces, contours for a different pre-defined variable can be made. If required user-defined variables can be defined if required and comparisons can be done easily for flow conditions.

Advantages of CFD

i.) Make a model to work at real conditions which are difficult in experimental models.
ii.) CFD can perform analysis at high speed with a negotiable error.
iii.) The cost of simulation is reduced and we can change geometry as many as time till the most appropriate result is obtained.

Limitation of CFD

i.) Results totally depend on the physical model so we must form it correctly.
ii.) The accuracy of the model depends on given initial and boundary conditions.

1.8 Objective of study

To study the flow pattern in groyne field with depth:-

iii.) To study the variation in protection length, the width of separation zone with different Froude Number, the shape of the groyne.
iv.) To study the development of flow with depth around the groyne field.

v.) Variation in bed shears with Froude Number, the shape of the groyne.

vi.) To study the effect of groyne shape on the mechanism of the horseshoe vortex (HSV).

1.9 Scope of the project

Present investigation focuses on analysing the flow around a single groyne with different alignment and shape for varying Froude Number. Protection length can be a deciding factor for installation interval in a series of groynes, bed shear stress value in groyne field can be used to determine the zone of the high potential of scouring. Study of sediment transport around a spur-dike can be done by analysing the shear stress at bed level of the channel.

The result of the study will help us in deciding the best alignment & shape of groyne for different Froude Number so that destabilisation factor can be minimized.

vii.) ANSYS FLUENT 16.0 is used throughout the project to study & visualise the flow around the groyne, variation in velocity w.r.t. initial velocity, separation or protection length, dynamic detached shear layer (DSL), bed shear variation in the vicinity of groyne has been visualized. Fluent contain many models for turbulent flow analysis, but in the present study, we use PRESTO model to analysis the flow to get better results.

Chapter-2

LITERATURE REVIEW

Mukesh Raj Kafle et al. [5]

Study employ a numerical model NAYS 2D to simulate flow near groyne in fixed flat-bed. Cubic interpolated pseudo particle (CIP) method used as a finite differential method for advection. Turbulence closure, eddy viscosity model, k-ϵ model and zero equation model used and compared to statistical parameters. By the comparison k-ϵ model is found superior over rest of two models.

Daniel S. Hersberger et al. [6]

Effects of vertical ribs, placed as a macro-roughness element on the outer vertical wall of 90^{o} laboratory channel bend, investigated the impact on bed morphology and in the form of flow velocity field. The result of time averaged velocity showed macro-roughness in outer bank make maximum velocity cell, observe near the outer bank for smooth outer walls moves towards the center of the channel. High longitudinal velocity is shifted towards the inner wall by a distance of about one times the mean flow from the outer wall.

Francis et al. [7]

performed various experiments in a rectangular flume to study the downstream recirculation zone but they did not measure the velocity. They found that the length of eddy zone is chiefly dependent upon the relative size of the spur, and independent of face angle, form of spur, or sweep angle in the normal range.

Rajaratnam and Nwachukwu [8]

performed experimental studies on the structure of turbulent flow near groyne like structures. They analysed the deflected flow using the model of the three dimensional turbulent boundary layer. They used thin plate groynes as well as semi-cylindrical hose groyne for analysis.

Ouillon and Dartus [9]

performed a 3D numerical simulation of a steady, shallow turbulent flow around a groyne in a rectangular channel. They compared isolines of water depths and mean velocity fields with

experimental data. They analysed the results of pressure field, shear stress distribution and turbulence

Mioduszewski et al. [10]

studied the influence of the structure permeability on flow pattern and local scouring process near a groyne. The parameters which leads to scouring were of smaller intensity for permeable groyne than impermeable groyne. Seepage force was not seen in case of permeable structure.

Ettema and Muste [11]

performed a series of flume experiments to determine the scale effects in small scale models of flow around a single spur dike placed in a fixed and flatbed channel. The parameters they studied were flow-thawleg alignment(line of maximum streamwise velocity) and area of extent of recirculation zone. They showed that use of a shear stress parameter as the primary criterion for dynamic similitude influences these parameters.

Uijttewaal [12]

performed experiments in physical model of a river reach geometrically scaled to 1:40. Four different types of groynes were tested and all of them were arranged in an array of five identical groyne fields. Flow velocities were measured using PTV. The design of experiment was such that the cross sectional area blocked by the groyne was same in all the experiments. The experimental data were used to understand the physical processes like vortex formation and recirculation zone.

Yeo et al. [13]

performed 69 experiments in a flat and fixed open channel with groynes made of acrylic of different permeabilities, relative lengths approach velocities. He changed the permeability of groynes by providing gaps between the acrylic cylinders. The tip velocity of the groyne were measured with the acoustic dopple velocimeter(ADV). The two dimensional velocity field were measured with large scale particle image velocimeter(LSPIV) technique. He suggested an empirical equation for tip velocity in terms of approach velocity and groyne area ratio. He also suggested an empirical equation describing the relationship between the ratio of the separation length to groyne length and Froude number.

Xuelin et al. [14]

used large eddy simulations to model the three dimensional flows around a non-submerged spur dike. The finite volume method was used to discretize the Navier-Stokes equations, and the SIMPLEC algorithm was used to solve them. The computational results were in good agreement with experimental results.

Ho et al. [15]

performed numerical modelling in FLOW-3D software for single groyne in a rectangular flume to investigate flow pattern changes and to find the best performing installation interval. He developed numerical model for the experiments performed by Yeo et al [27].

McCoy et al. [16]

performed a Large eddy simulation(LES) on the groyne field in a straight open channel. The mean velocity at the free surface was found to be in good agreement with the experimental results. The bed shear stress was found to be more in the region close to downstream of the groyne.

Duan [17] experimentally studied the three dimensional turbulent flow field around a spur dike in a fixed bed open channel using a microacoustic dopple velocimeter. Mean and turbulence characteristics were evaluated upstream and downstream of the spur. The maximum bed shear stresses estimated using Reynolds stresses were about three times the mean bed shear stresses of the incoming flow.

Safarzadeh et al. [18]

performed experimental measurements to investigate the head shape effects on bed shear stress distribution around single straight and T-shape groynes. Distribution of shear stress was more uniform downstream of the T-shape groyne.

Chapter-3

METHODOLOGY

3.1 Numerical method

The rectangular channel with the single groyne of different shape & alignment is analyzed using ANSYS FLUENT 16.0. the process of the simulation of flow involves generally these three steps:-

a.) **Pre-Processing**

i.) Defining a geometry and flow domain.

ii.) Specifying flow conditions (laminar, turbulent etc.).

iii.) Defining initial & boundary conditions.

b.) **Solver**

Iterations are done over and over till desirable level of accuracy is attained.

c.) **Post Processing**

Results are analysed by forming contours, vector field, streamlines, charts and graphs between the various variable in the flow domain.

3.2 Preparing a Model

ANSYS software provides us with a platform for design, meshing geometry, solving and then results are visualized in the form of streamlines, contours, volume rendering, graphs, particle track, vector.

3.3 Geometry setup

ANSYS Workbench is embedded with geometry defining element known as Design Modular. Where we can make the required geometry like in our case channel and groyne. In Design Modular we can also define the boundaries of a geometry like an inlet, outlet, bed surface, side walls etc.

The dimension of the channel is 6.515mX0.4mX0.15m. For our study are going to place five different groyne one by one at 2m from the inlet. All of these are non-submerged type groynes. Out of these five groynes:-

i.) A straight groyne of length 5cm.

ii.) Two are repelling type groynes making an angle of 60° and 45° with the upstream bank and both are of 5cm length.

iii.) Two are special shape groyne

a.) T-shape groyne with full wing length.

b.) T-shape groyne with half wing length.

The thickness of all groynes is 1.5cm. In the current study, we stimulate the flow arranged the groyne field for different Froude number.

Table 3.1 - The Experimental Cases

Serial no.	Type of groyne	Θ	Length in plane view (cm)	symbol
1.	Deflecting	90°	5	SD-5
2.	Repelling	45°	5	RG-45-5
3.	Repelling	60°	5	RG-60-5
4.	T-shape		Full wing length	TF
			Half wing length	TH

3.4 Flow characteristics

The flow characteristics in all types of the geometry were divided into two

Table 3.2: The flow characteristics

	Case 1	Case 2
Uniform flow depth (d)	10.5cm	10.5cm
width of flume (B)	40.0cm	40.0cm
Discharge (Q)	0.01942m^3/sec.	0.01456 m^3/sec.
Mean velocity (v)	0.37 m/sec.	0.2775 m/sec.
Channel bed slope (S_o)	0	0
Froude Number (Fr)	0.364	0.2732

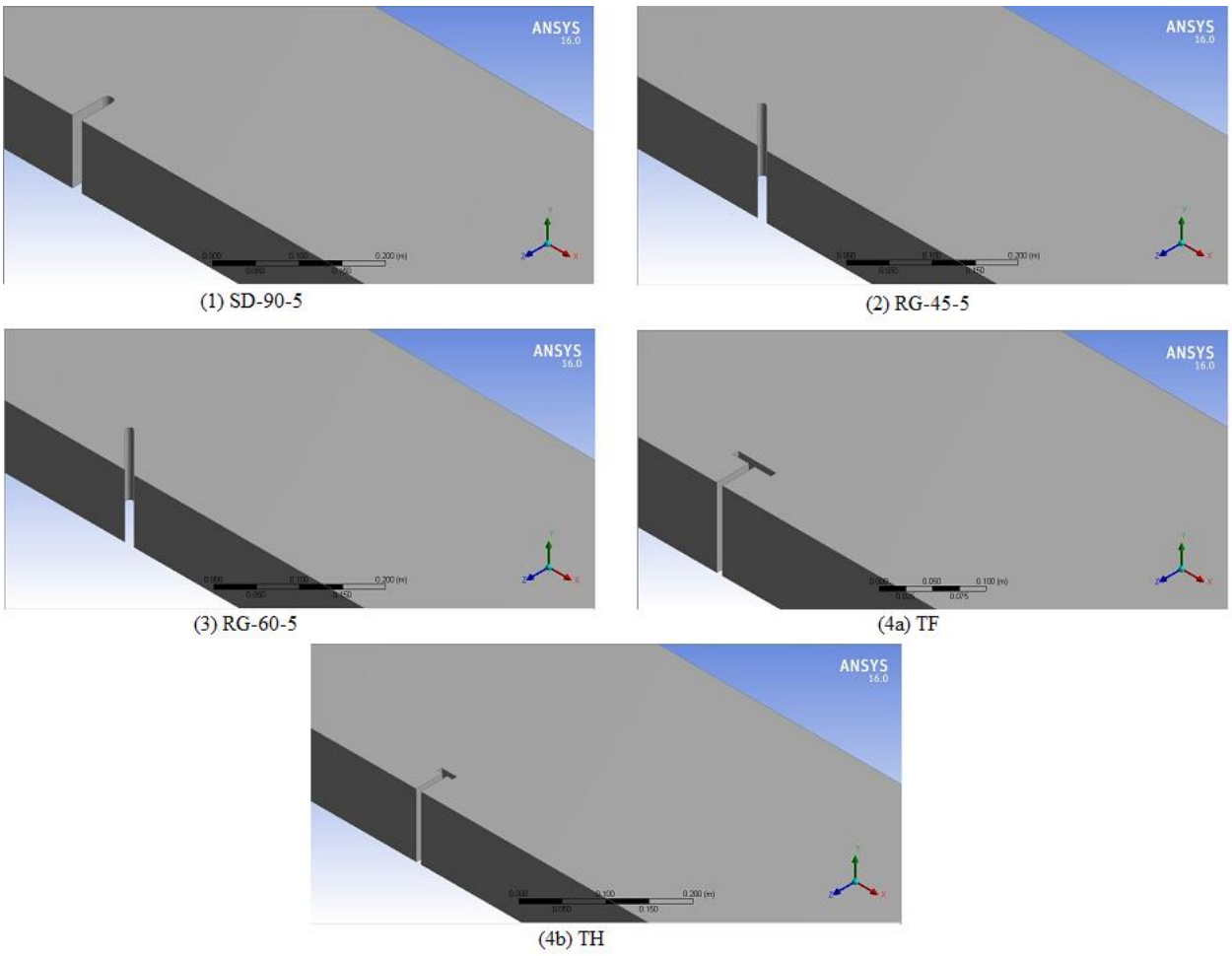

Fig. 3.1 various geometry of channel with groyne prepared using Design Modeller

3.5 Meshing

ANSYS workbench also has its own meshing tool. Meshing of all models is done separately. During meshing "Proximity and Curvature" is opted for "advanced size function". For "Relevance center" "fine" is opted & "high" is selected for "smoothing". In "assembly meshing method", "tetrahedrons" is selected. The maximum size of cell edge is limited to 1.19e-02m. A total tetrahedral cells in which whole geometry is divided is in the range of 13,00,000 to 13,50,000.

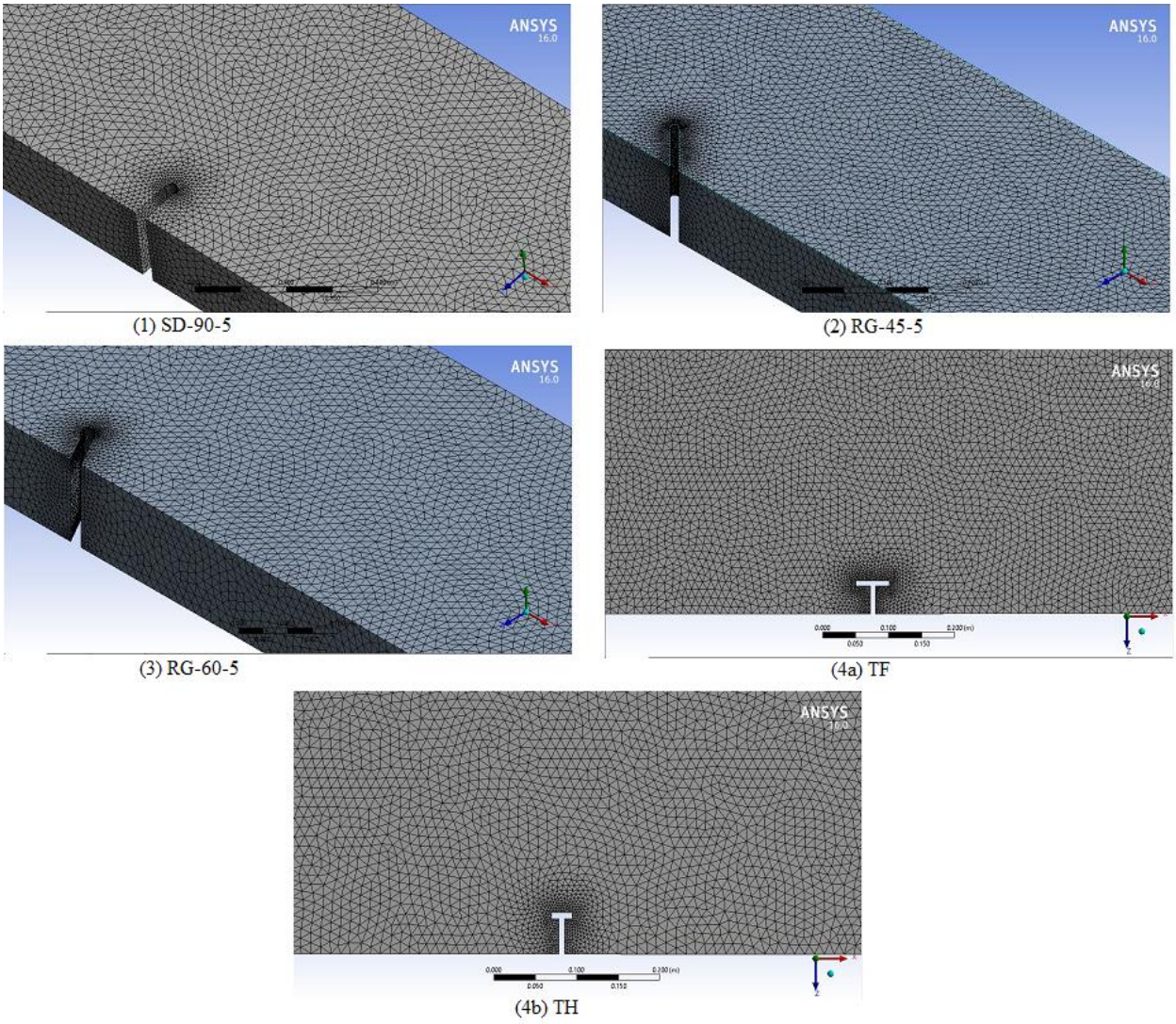

Fig. 3.2 Meshing of geometry is done using meshing tool of ANSYS Fluent 16.0

3.6 Fluent Setup

Fluent setup is consists of these steps

1. **Define operating condition**

   Operating pressure is specified equal to zero at the top of the inlet as we assume that water is not going to overtop the side walls of the channel. Gravity is also specified to negative 9.81 m/sec^2 in y direction & in the last specific operating density value is loaded equal to zero. As shown in below fig.

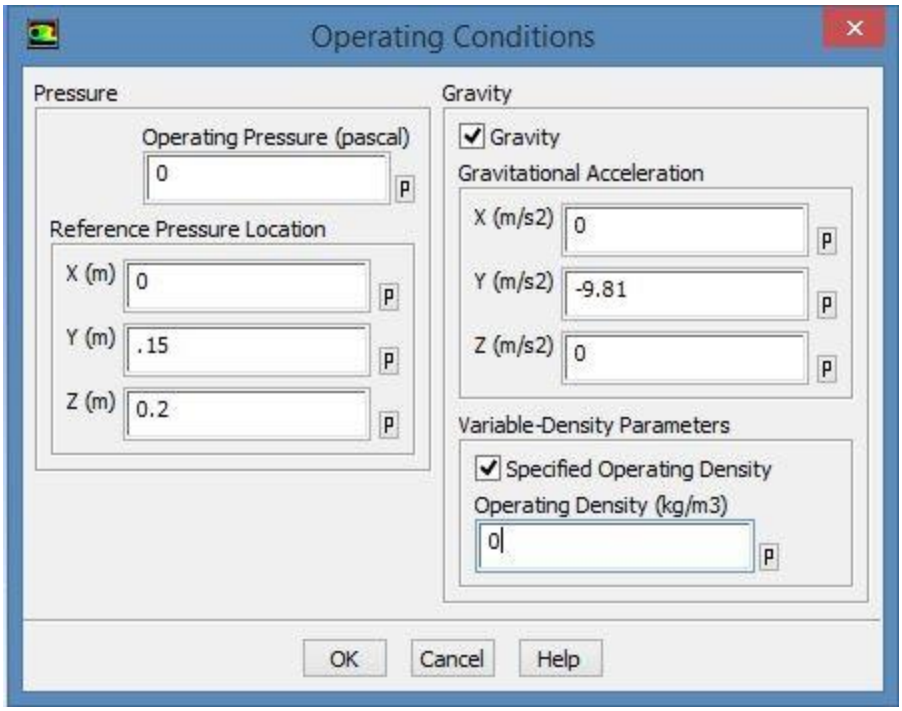

Fig. 3.3 operating conditions defined in FLUENT Setup

2. **Define material**

   In the default setting, we have only air as fluid in the material so we add water from the fluent database.

3. **Define model**

   a.) Multiphase model is defined by marking a "volume of fluid", the formulation is Implicit Body Force. In VOF Sub-model Open Channel opts.

   b.) For Viscous Model k-epsilon (2 equation) is selected with realizable. Near-wall treatment is Non-equilibrium wall functions. Curvature correction is also marked. Other fields are kept as default.

   c.) Reynolds-averaged Navier-Stokes Equation also known as k-epsilon equation for representing turbulence characteristics to determine eddy-viscosity by finite volume method.

   d.) In k-epsilon (2 equation), equation consists of ReynoldsAveraged continuity equations and incompressible equation and incompressible Navier-Stokes Equation.

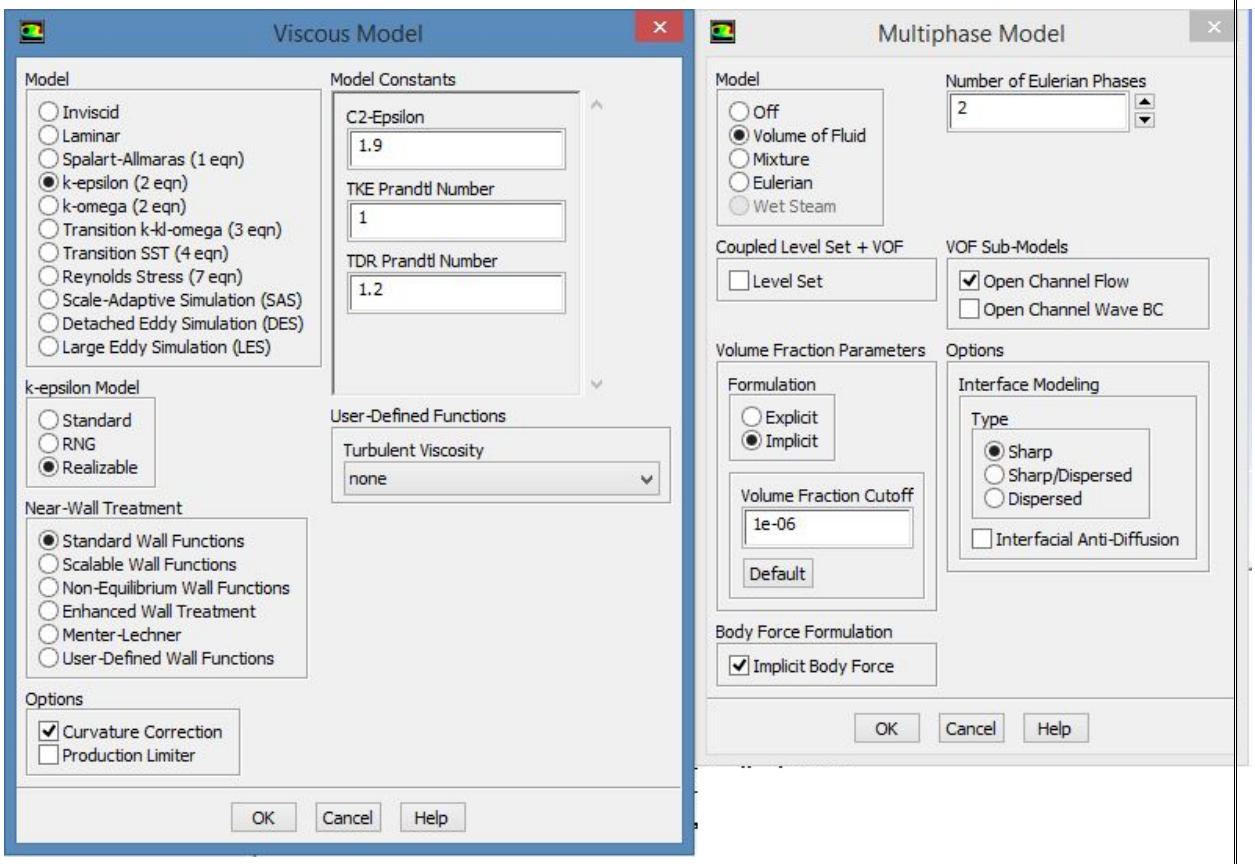

Fig. 3.4 Model defined

4. **Water is selected as primary phase & air as secondary.**
5. **Boundary conditions**

   The inlet is kept as pressure Inlet. In Multiphase open channel is marked & Depth of flow is given equal to 10.5 cm. In Momentum velocity is given equal to a.) 0.37m/sec. & b.) 0.2775m/sec.

   Turbulent Intensity % is kept 10 & turbulent viscosity ratio is 100.

   For side wall and bed surface, no slip condition & stationary wall is marked. For outlet Pressure Outlet & in multiphase gauge pressure is specific as zero at the outlet.

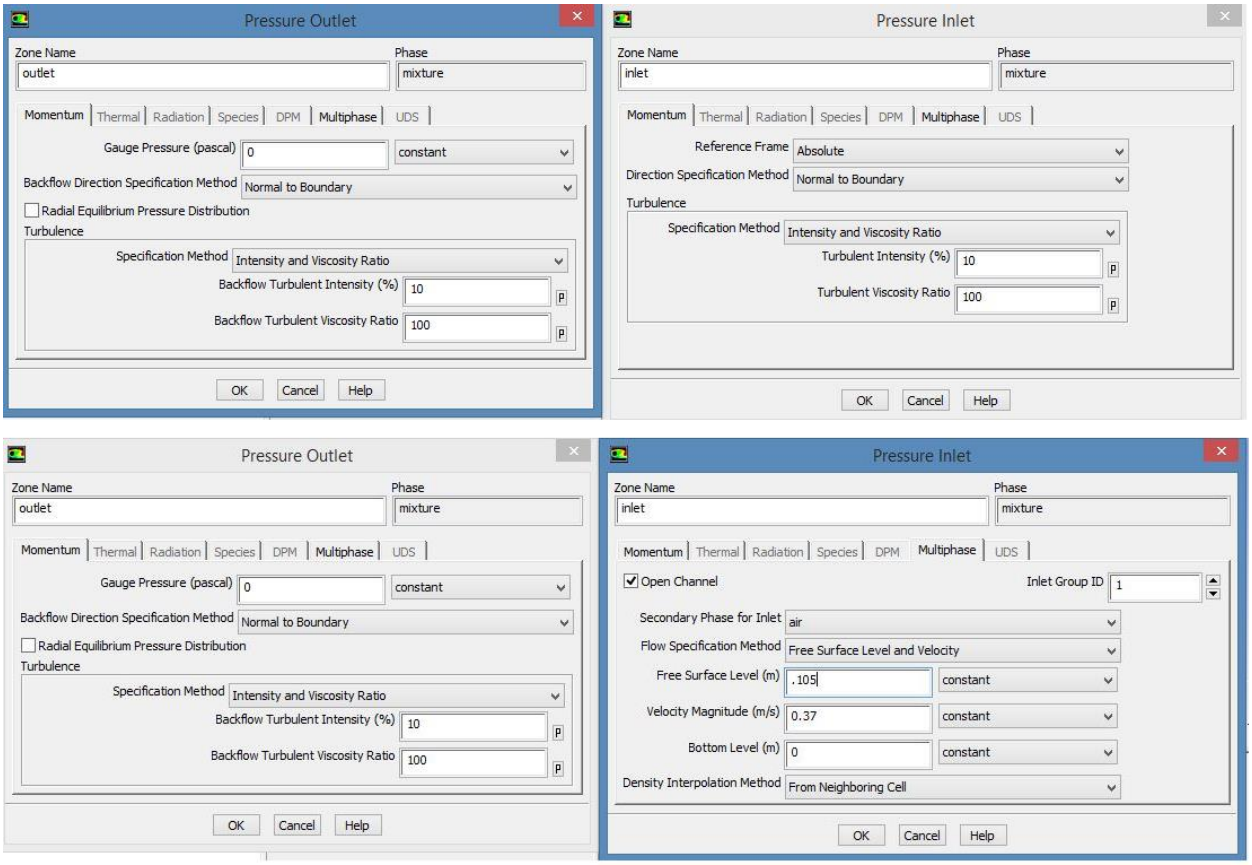

Fig. 3.5. Boundary condition at inlet and outlet

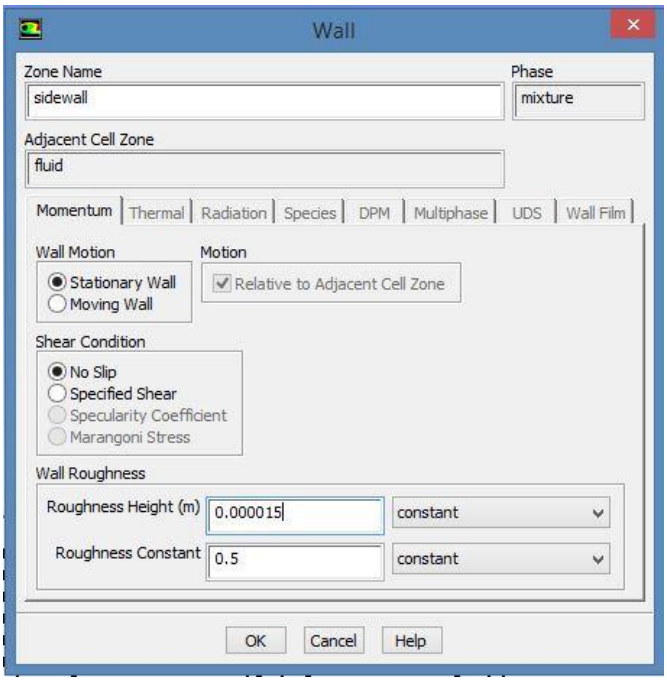

Fig. 3.6. Boundary condition for side wall, groyne, bed surface

6. Here we use “PISO” Solution method scheme and “modified HRIC” for volume fraction in spatial discretization. Modified HRIC and BGM are best to choose but as BGM method is time-consuming here I use modified HRIC.
7. Before start calculation, initialization is done and the solution is computed from “Inlet”.
8. 1500 iterations are done for each run.

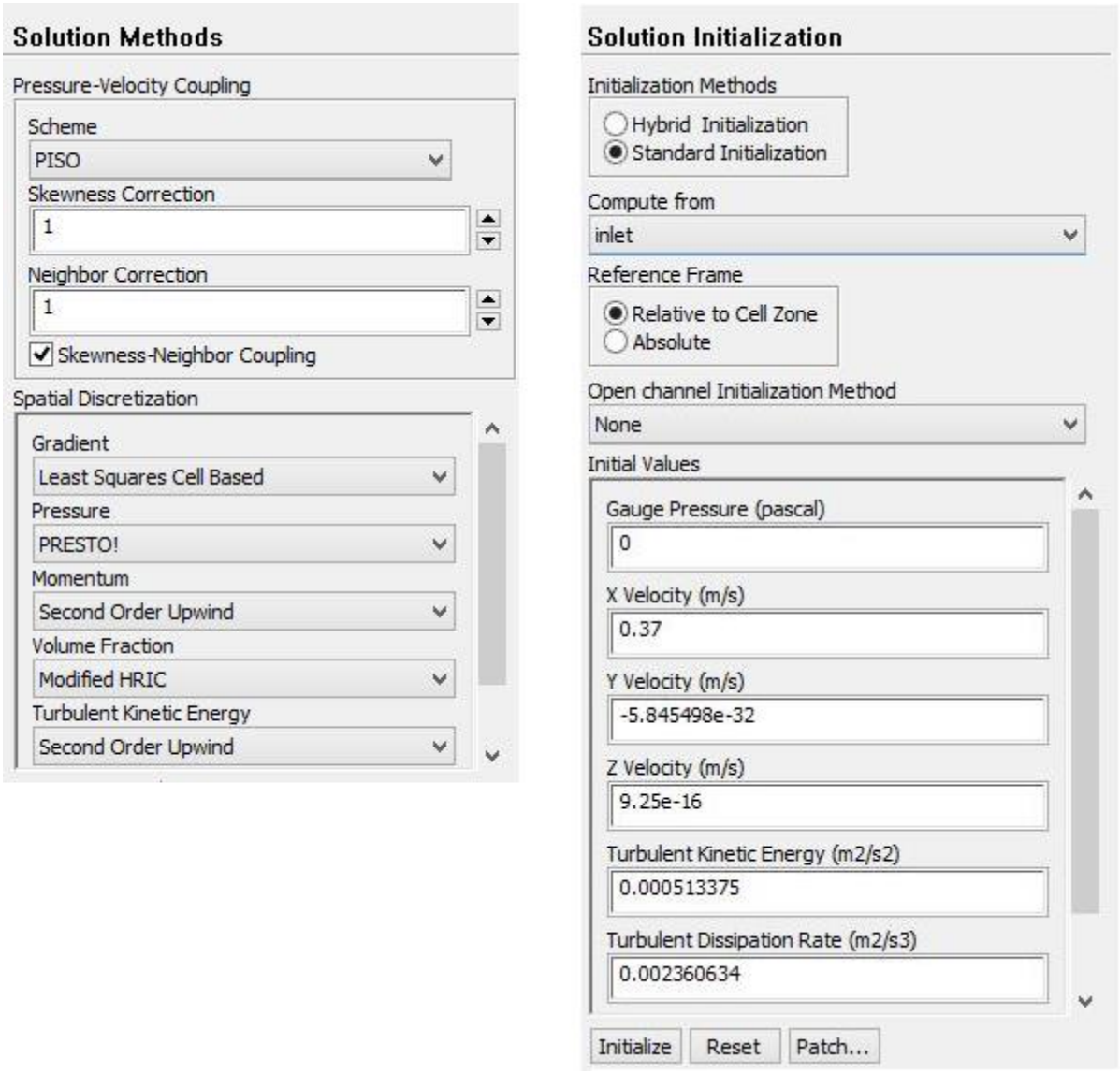

Fig. 3.7. left snapshot “Solution Method” & right snapshot “Solution Initialization”

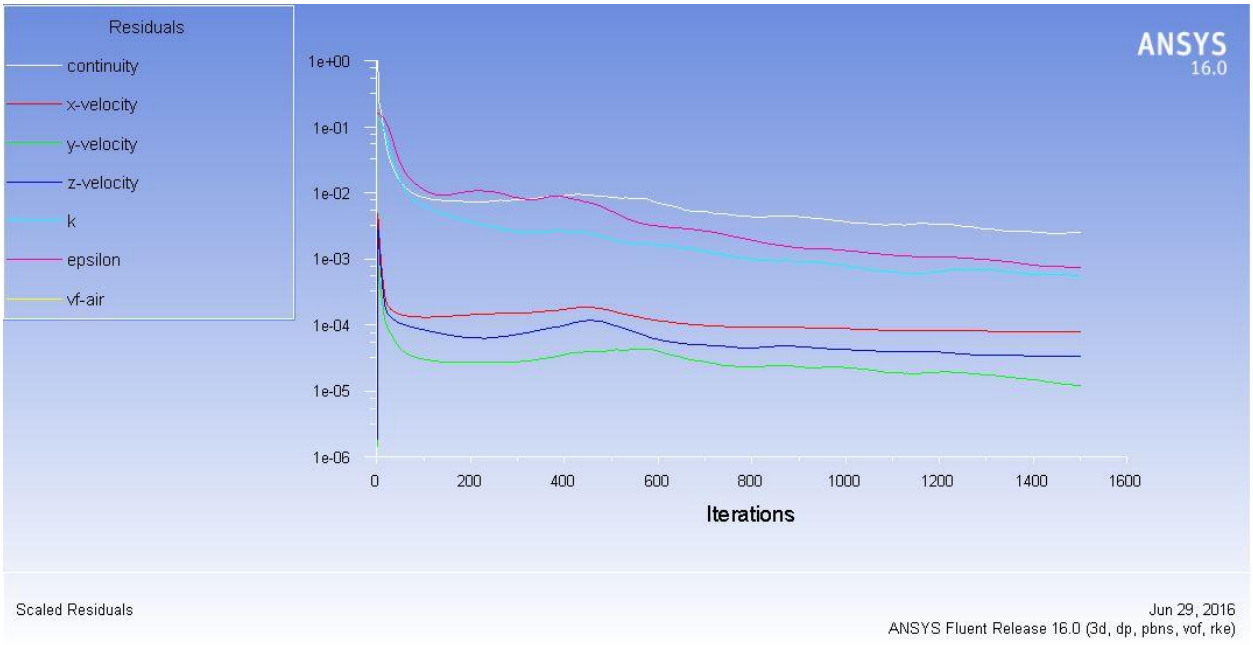

Fig. 3.8 residuals after 1500 iterations in the case of SD-90.

Chapter-4

RESULTS AND DISCUSSIONS

Velocity analysis and data post-processing performed using CFX post tool of ANSYS Workbench. Contour are plotted of :- different time-averaged velocity vectors, streamlines, and flow data is prepared at various planes using measured data points cloud. Here firstly general flow features are presented, then detail flow structure such as HSV system and DSL are analyzed, protection length & width of recirculation zone is also analyzed.

4.1 General Flow Patterns

Two horizontal planes are consider as point of interest

a.) Near the bed region just above the fully developed boundary layer.

b.) At near water surface, where maximum flow velocity is observed.

Average of Z/H for different shape of the groynes is comes out equal to

For near bed region Z/H = 0.035

For near water surface plane Z/H = 0.58.

1. At two horizontal planes (Z/H ≈ 0.035 and 0.58) time averaged flow streamlines are prepared and shown in fig. 4.1 and 4.2 for different tested groynes arrangements and shapes. The horizontal vector field in a detailed manner is also shown in fig. 4.3 and 4.4.
2. Flow pattern varies with depth, upstream of the groynes. Flow structure is prominent different in T-shape and straight & repelling type groyne.
3. The Z/H ≈ 0.58 surface streamlines smoothly bends towards the groyne tip [fig. 4.1(b) and 4.2(b)] as the flow reaches the immediately upstream section of the SD but a back-flow near the junction of groyne and the side wall is seen in near bed velocity vectors [fig. 4.3(a) and 4.4(a)]. So, from this, a strong traverse flow is depicted near the tip on near bed plane. Same kind of flow structure can be seen in the case of the repelling type of groynes.
4. Formation of a prominent and more stable circulating flow in the T-shape case at Z/H ≈ 0.58 surface is the main difference between the T-shape, straight and the reflecting type of groyne, just upstream of the groyne [Fig. 4.1(h), (j) & Fig. 4.2(h), (j)].

5. Mean flow at the tip of the groyne in case of TH & TF is weaker in this region then the straight one additionally a clockwise rotational flow is formed at G-S junction.[fig. 4.3(j) and 4.4(j)]
6. Circulation zone sufficiently develops in depth and occupy the whole zone block between upstream face of groyne and upstream part of the wing segment as we increase the length of the wing (i.e. TF case) [Fig. 4.3(h) and 4.4(h)].
7. By comparing velovectors of both repelling type groyne & SD it is found that there is no difference nature of flow as we discuss before for different depths but as smaller the angle of repelling groyne stronger is the backflow.

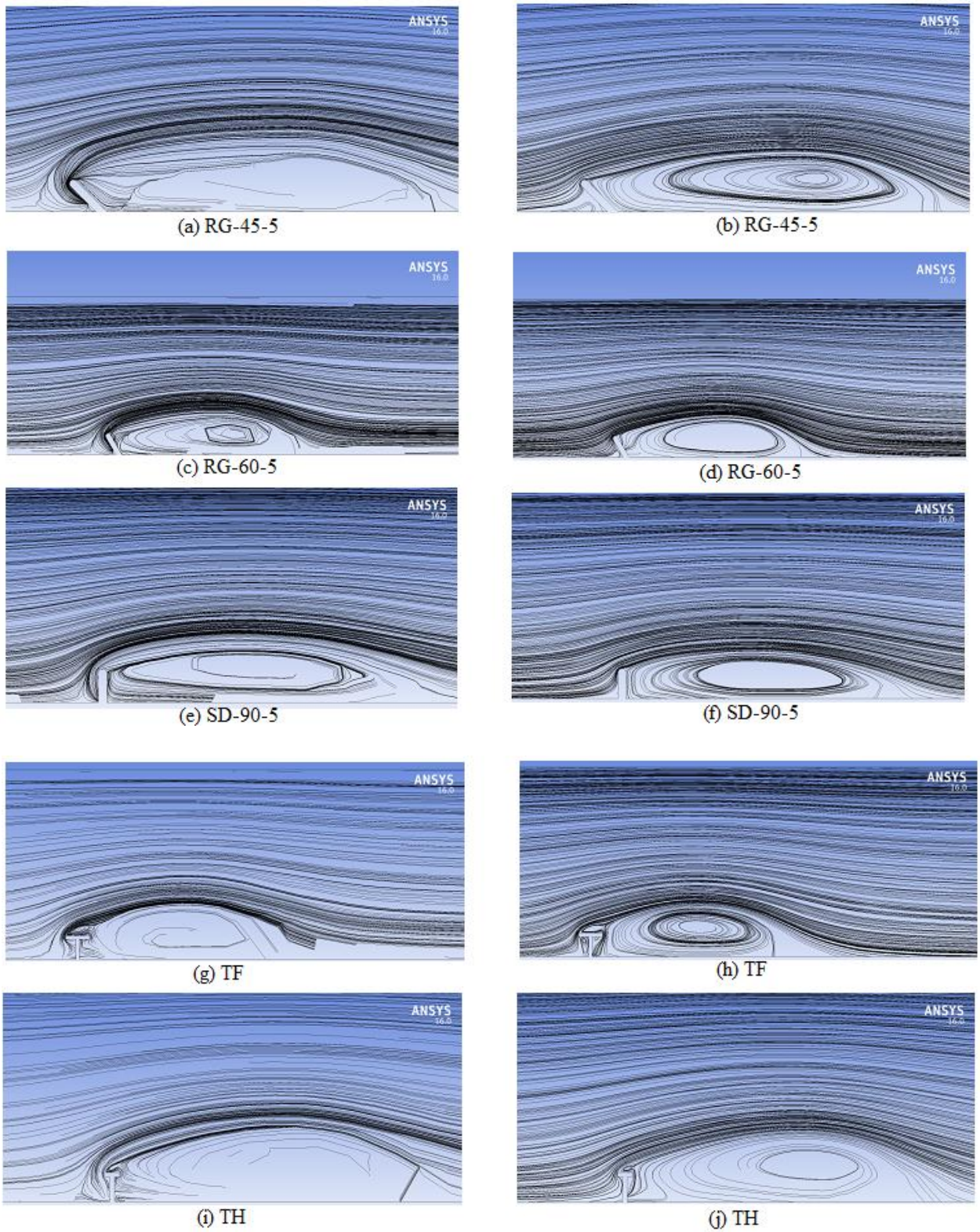

Fig. 4.1. Case 1. Fr. No. = 0.364. Mean flow features at different horizontal planes for various tested groynes: (a, c, e, g, and i) streamlines at (Z/H = 0.035) planes; (b, d, f, h, and j) streamlines at (Z/H = 0.58) planes

8. The value of Froude number has a negligible effect on the flow structure for all the shape & alignment for both depths of consideration.
9. The vertical pressure gradient immediately upstream of the straight & repelling type groyne push near bed fluid toward groyne tip and due to which a strong traverse flow occurs. However, in special type groyne (T-shape groynes) the upstream wing segment laterally block the upstream part of spur-dike and prevent the formulation of traverse flow to the head of the groyne. Mechanism of HSV at the base is also strongly affected by wing segment which discussed in detail later.

Fig. 4.2. Case 2. Fr. No.= 0.2732. Mean flow features at different horizontal planes for various tested groynes: (a, c, e, g, and i) streamlines at (Z/H = 0.035) planes; (b, d, f, h, and j) streamlines at (Z/H = 0.57) planes

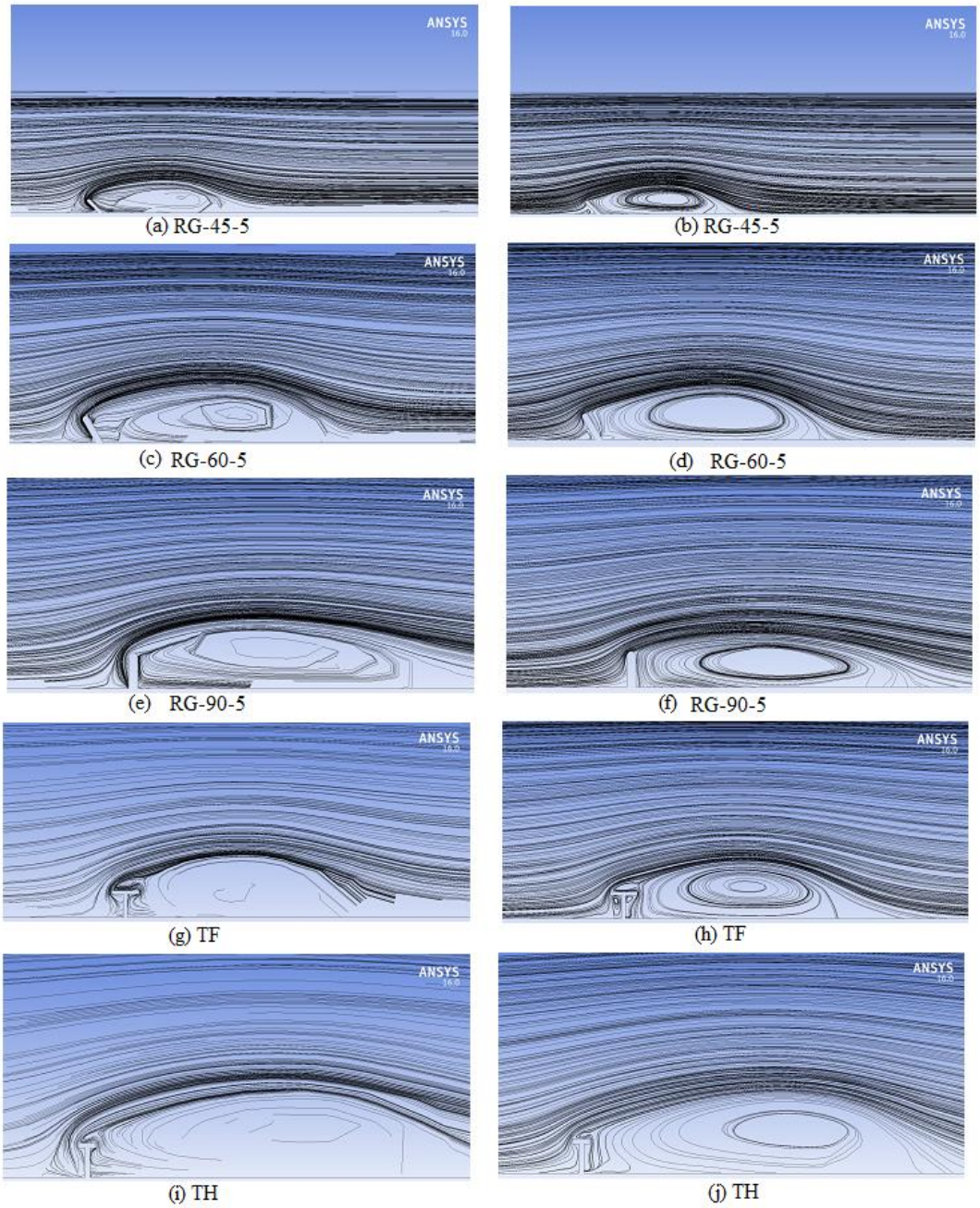

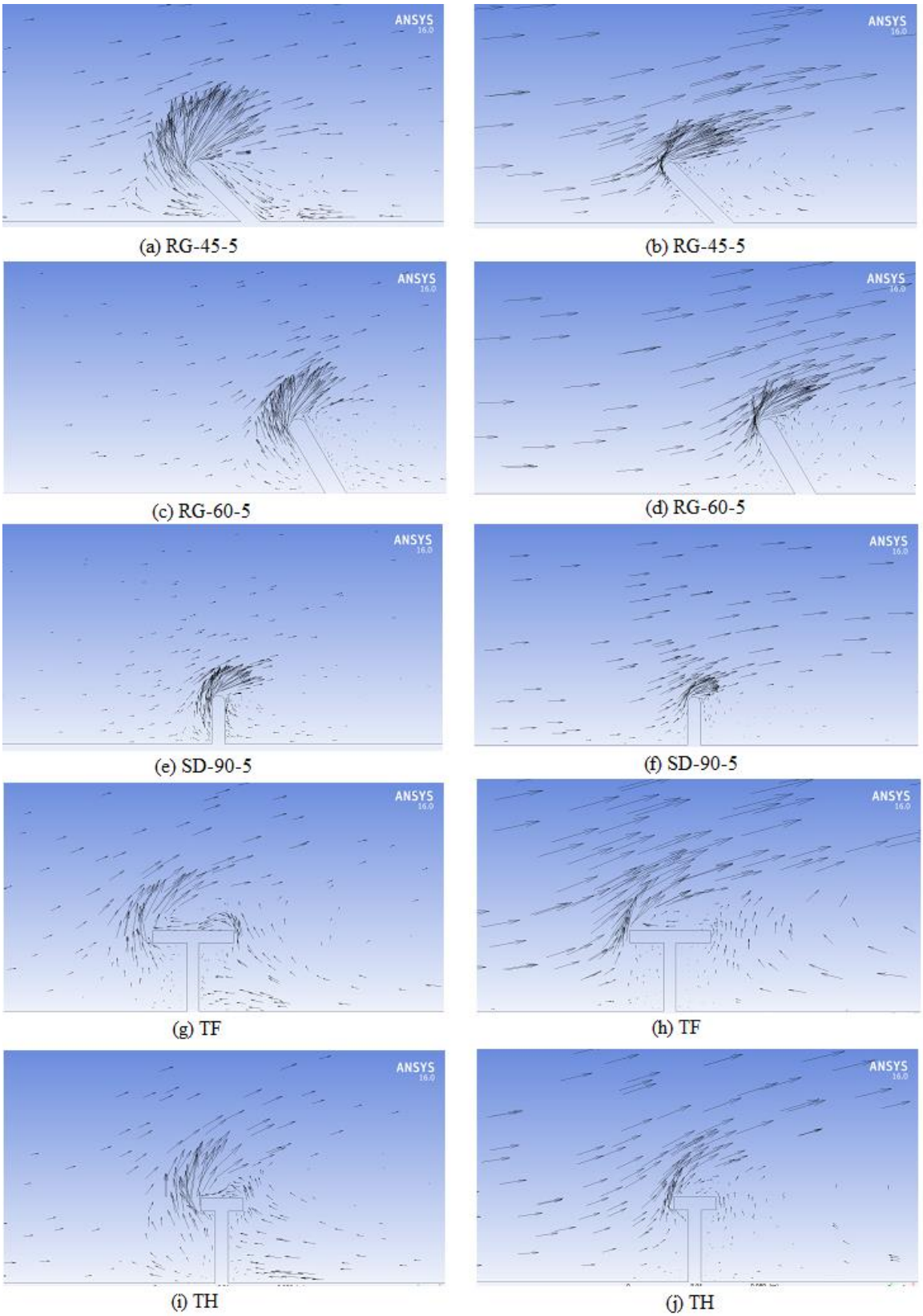

Fig. 4.3. Case 1. Fr. No. = 0.364. Velocity vector at different horizontal planes for various tested groynes: (a, c, e, g, and i) (Z/H = 0.035) planes; (b, d, f, h, and j) (Z/H = 0.58) planes

Fig. 4.4. Case 2.Fr. No. = 0.2732. Velocity vector at different horizontal planes for various tested groynes: (a, c, e, g, and i) (Z/H = 0.035) planes; (b, d, f, h, and j) (Z/H = 0.58) planes

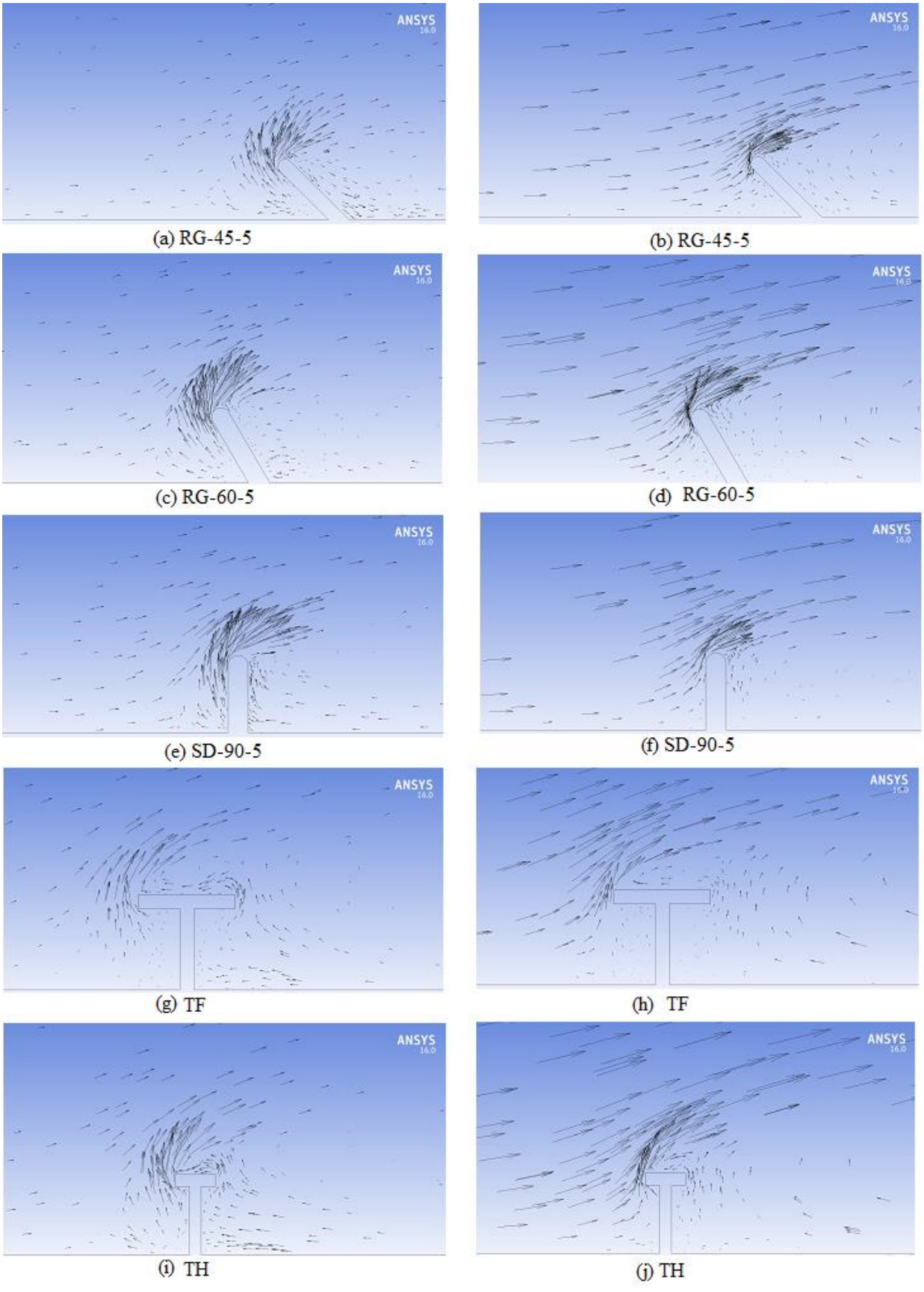

(a) RG-45-5 (b) RG-45-5

(c) RG-60-5 (d) RG-60-5

(e) SD-90-5 (f) SD-90-5

(g) TF (h) TF

(i) TH (j) TH

4.2 Recirculation Zone

By combined evaluation of velocity streamlines at near bed surface & near water surface plane and bed shear contours. The following table is prepared of downstream protection length of different studied groyne & width of recirculation zone.

Table 4.1 Streamwise and lateral extends of the main recirculation zone for different groynes

	Groyne type	X_r/L		Y_r/L	
		Near water surface plane	Near bed plane	Near water surface plane	Near bed plane
Case 1	SD	11.9	11	1.9	1.4
	RG-45	12.8	13.4	2.4	2
	RG-60	12.1	11.8	2.1	1.8
	TH	11.2	10.9	1.7	1.6
	TF	9.1	10	2	1.8
Case 2	SD	12	11.2	2.1	1.6
	RG-45	12.6	13.2	2.3	1.9
	RG-60	12	11.6	2	1.6
	TH	11.1	11	1.8	1.6
	TF	8.8	9.6	1.9	1.8

Dimensionless Dynamic Shear Layer (DSL) reattachment length or protection length (X_r/L) and maximum lateral extend of the main separation zone (Y_r/L) for various tested groynes are noted in the table. Protection length (X_r/L) for any horizontal surface is taken as the point where the streamwise velocity near the sidewall is equal to zero.

In the case of the straight groyne, the protection length near bed surface is less than that near water surface plane but in the case of TH they are very close & in the case of TF near bed length is longer than that of near water surface.

By comparison, (X_r/L) at Z/H = 0.58 plane it is found that the decreasing order of protection length for the different shape of groynes is RG-45>RG-60=SD>TH>TF.

Y_r/L difference in two planes of study for straight is equal to 0.5 but in the case of TH & TF at both planes the values of Y_r/L is approximately equal. This effect is attributed due to the effect of the upstream part of the wing segment in T-shape groyne. The position of the center of recirculation zone moves upstream by going from SD to TH. The angle of the groyne is less, nearer is the centre of recirculation zone to the groyne. Correct increasing order of distance of centre of recirculation from groyne zone in different cases is [RG-45; RG-60; SD-90; TF; TH]. The measured reattachment length for SD case conforms to previous observations [eg Akbar Safarzadeh 2016, Rajaratnam and Nwachukwu 1983].

From the table it can be easily depicted that there is no major effect on protection length as Froude Number varies.

Fig. 4.5. Contour of bed shear stress for different tested groynes; left plots: case 1 (Fr. No. = 0.362) and right plots: case 2 (Fr. No. =0.2732)

(a) RG-45-5

(b) RG-45-5

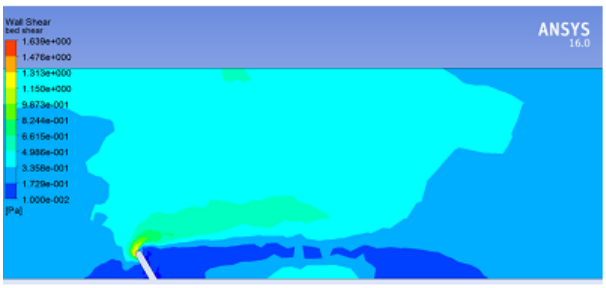

(c) RG-60-5

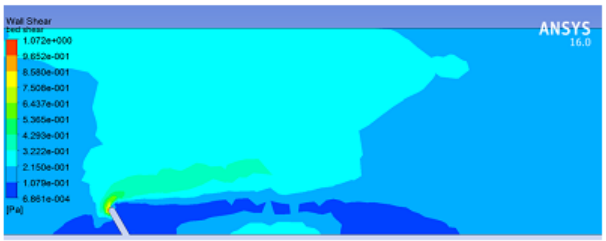

(d) RG-60-5

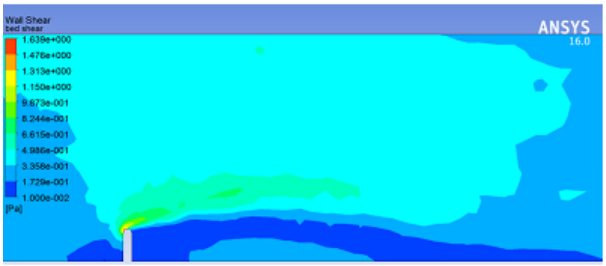

(e) SD-90-5

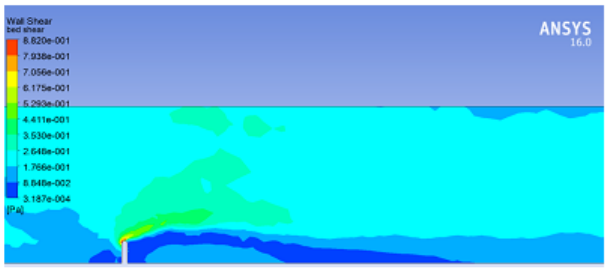

(f) SD-90-5

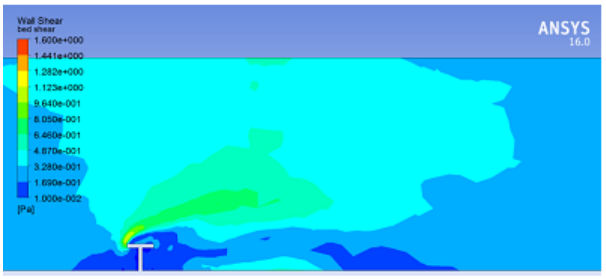

(g) TF

(h) TF

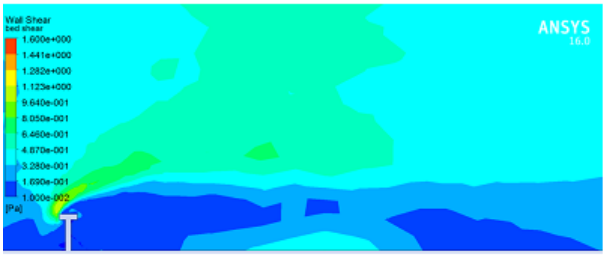

(i) TH

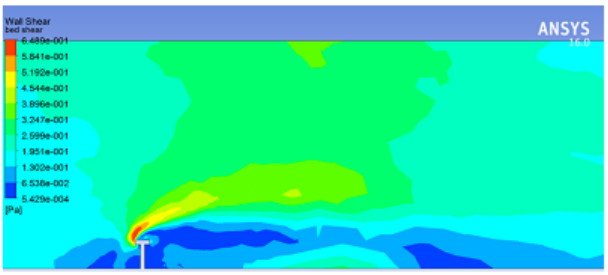

(j) TH

4.3 Velocity Variations

1. $U = (u^2 + v^2 + w^2)^{1/2}$, time-averaged velocity magnitude contours at $Z/H \approx 0.035$ and $Z/H \approx 0.58$ planes are shown in fig. 4.6. Two high-velocity zones, especially at near bed planes for various tested groynes, can be detected from all the contour plots.
2. Local effects of groyne structure cause a high-velocity zone [zone VA1 in fig 4.6(h)] because of spur-dike or groyne extrusion, another amplification of velocity occurs at the contracted area between the outer side of DSL & left bank of the channel.[zone VA2 in Fig. 4.6(h)].
3. Area of maximum velocity at the $Z/H \approx 0.58$ in each groyne is marked by black dotted lines.
4. At the upper layer in all cases, maximum velocity amplification occurs adjacents to the outer Dynamic Shear Layer (DSL).
5. The ratio between local maximum velocity magnitude and velocity of the approach flow at $Z/H \approx 0.58$ from this we can also validate with the previous experimental measurements (Molinas et al 1998) that show the vertical wall abutments are increased by up to 50%.
6. Velocity amplification at lower plane due to contraction of channel & local effect of the groyne is higher in the case of SD & RG-45 than other cases. This phenomenon is attributed high flow deflection in straight groyne and RG-45 compared with other groynes.
7. For higher length, the amplification is higher as the contraction effect dominates. So the amplification value is higher in such cases.

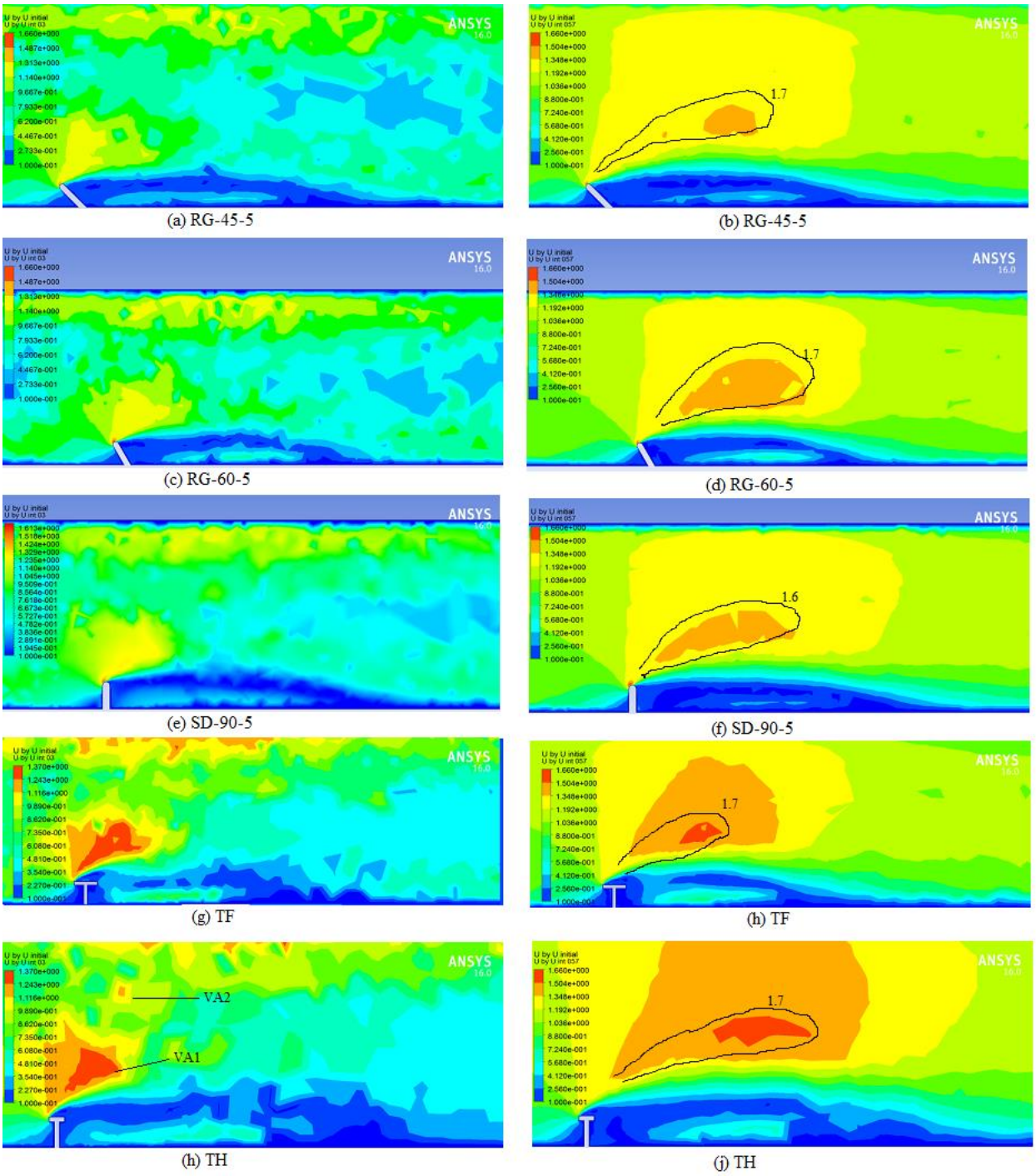

Fig. 4.6. Case 1. (Color) velocity magnitude contour (U/U_{in}) at different horizontal planes for various tested groynes; left plots: contours at (Z/H = 0.035) planes and right plots: (Z/H=0.58) planes

4.4 Vertical Velocity Component

1. Near bed planes around various test groynes, vertical velocity component contours are prepared & shown in fig. 4.7.
2. From fig. we can easily depict that the strong downward velocity contours are consolidated around upstream of the groyne tip. These velocities are the reason to the HSV, that forms in front of groyne & stoop(bend) in the direction of incoming flow from these vertical velocity contours at different planes revealed that HSV is limited to $Z/H<0.45$ layers.
3. Strongest downward flow is in the case of TF but wing shift the area upstream of groyne sufficiently. After T-shape strongest downward flow is in the case of SD.
4. In case of RG-45 a strong upward flow is seen at upward flow is seen at downstream side of groyne. This upward flow leads to scouring along the downstream base of groyne.

Fig. 4.7. Case 1. Vertical velocity component (w / U_{in}) distribution at ($Z/H = 0.035$) planes for various tested groynes

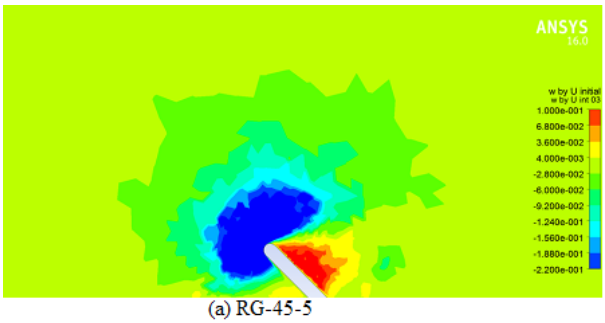

(a) RG-45-5

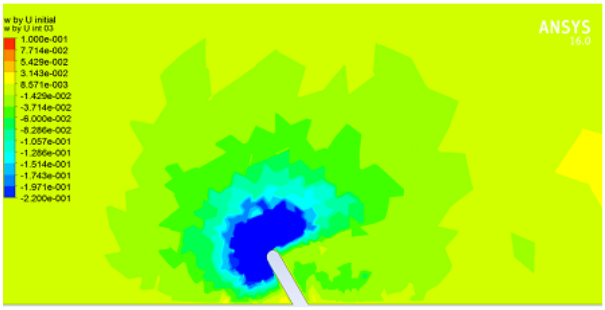

(b) RG-60-5

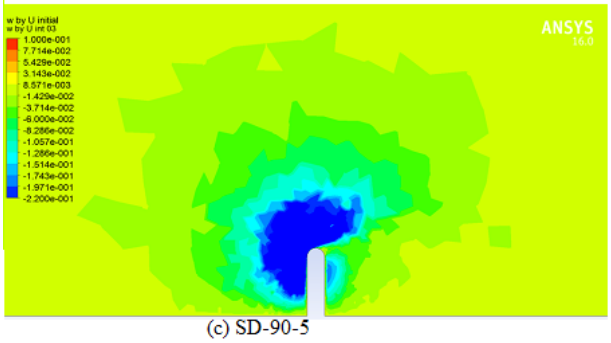

(c) SD-90-5

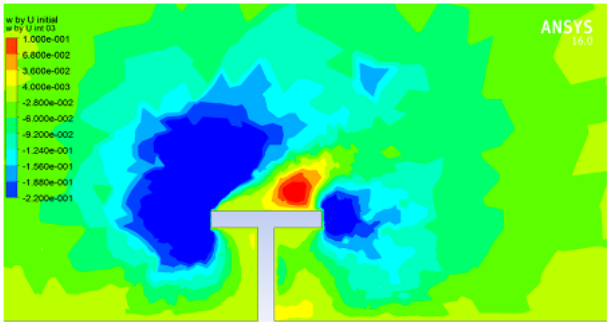

(d) TF

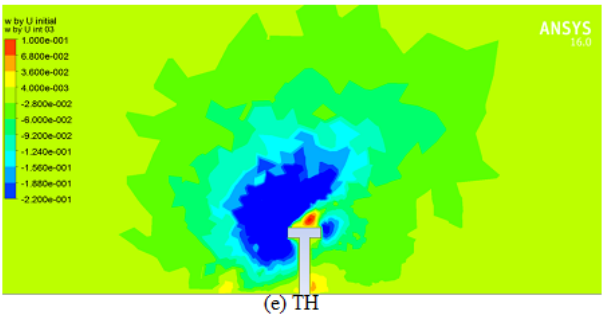

(e) TH

4.5 Streamlines at Various Vertical Plane

1. At different vertical planes (XY plane) upstream of groynes streamlines are presented in fig. 4.8. This fig. also contain the colour contours of fluctuations in root mean square (RMS) value of u velocity to initial inlet velocity of flow.
2. Rolling up of the incoming flow and separation of bed boundary due to reversed flow at the base are noticeable in SD.
3. Cross-section of HSV is elliptical & have clockwise rotation. The zone of a lower ratio of RMS u velocity & initial velocity coincides with the core of HSV being higher and more confined as Z/L increases.
4. Comparison of the streamlines between the T-shape, straight & repelling type groyne reveals that the wing segment of T-shape groyne has a considerable effect on the interaction between the approaching flow and the recirculating zone immediately upstream of the groyne. It is clear from fig. the separation point of the approach boundary layer moves upstream in TH and TF.
5. In all case except TF approaching flow is get separated & form a rotational movement. But in the case of TF flow is deflected towards channel bed and due to the wide, enough wing portion this downward flow is not able to get in contact with the approaching flow.
6. Due to which an interesting observation is come out that in the case of TF there is no Horseshoe Vortex (HSV). Results of which wing portion act as a scouring countermeasure.

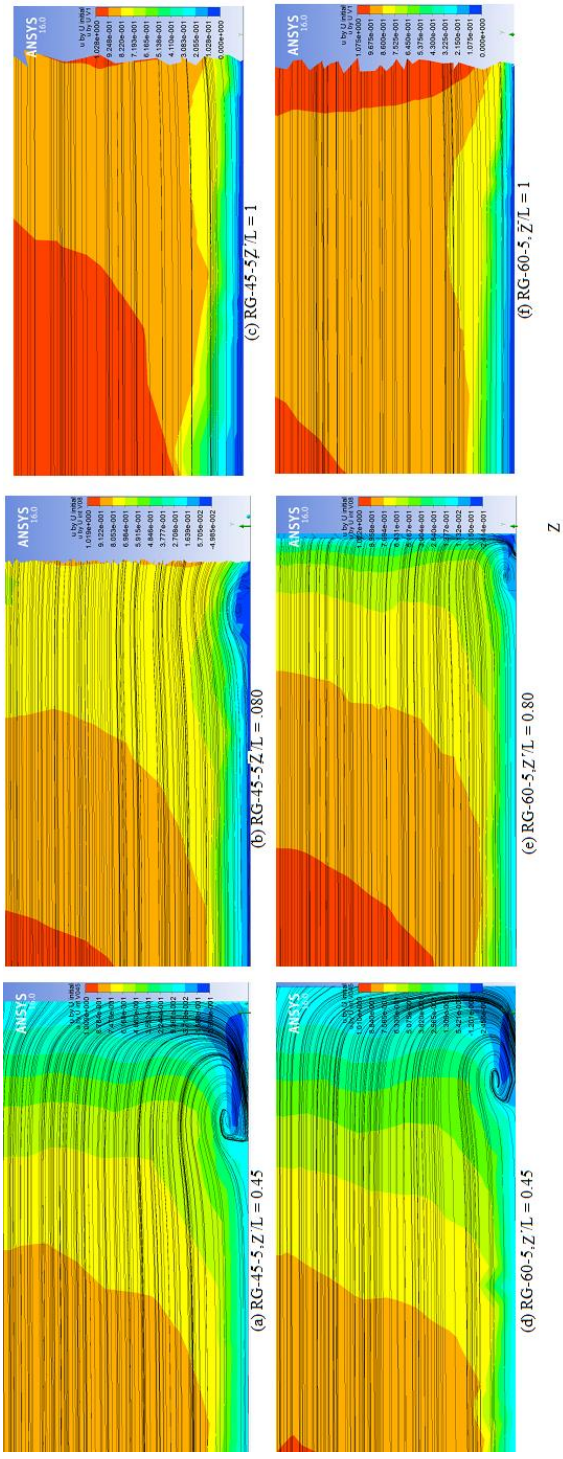

Fig. 4.8a case 1. Time-averaged streamlines at various vertical planes in front of the tested groynes; colour contour represents u'-RMS/U_{in}

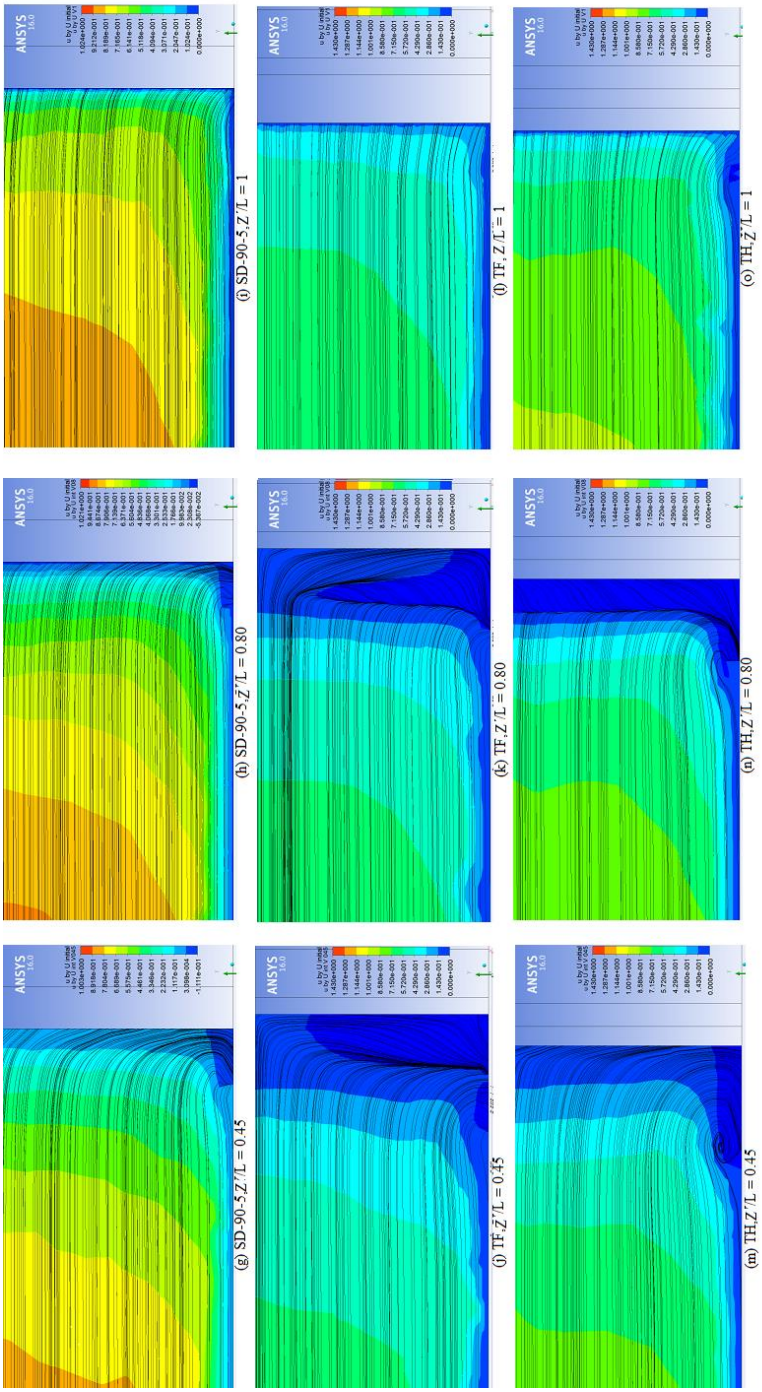

Fig. 4.8b.case 1. Time-averaged streamlines at various vertical planes in front of the tested groynes; colour represents u'-RMS/U_{in}

4.6 Turbulent Kinetic Energy

1. **TKE** = $0.5(\overline{u'^2} + \overline{v'^2} + \overline{w'^2})$

   u', v', and w' are fluctuations of velocity components and overbar signifies time averaged.
2. In fig. 4.9 averaged TKE increase is 10 times due to all types of the groynes.
3. As compared to the straight one TKE in the upper stream zone of T-shape groyne is higher due to the pressure of circulating 3D flow structures immediately upstream of T-shape groynes.
4. There is another highly turbulent zone around straight [SD] groyne in addition to the turbulence peak along the separated dynamic shear layer (DSL).
5. Fig. 4.9 shows the extension of this zone downstream of TH is less than SD one but in TF it is smallest among all.
6. Therefore it is evident from the fig.4,9 that along the DSL, TKE decreases much rapidly in T-shape groynes compared to SD one.

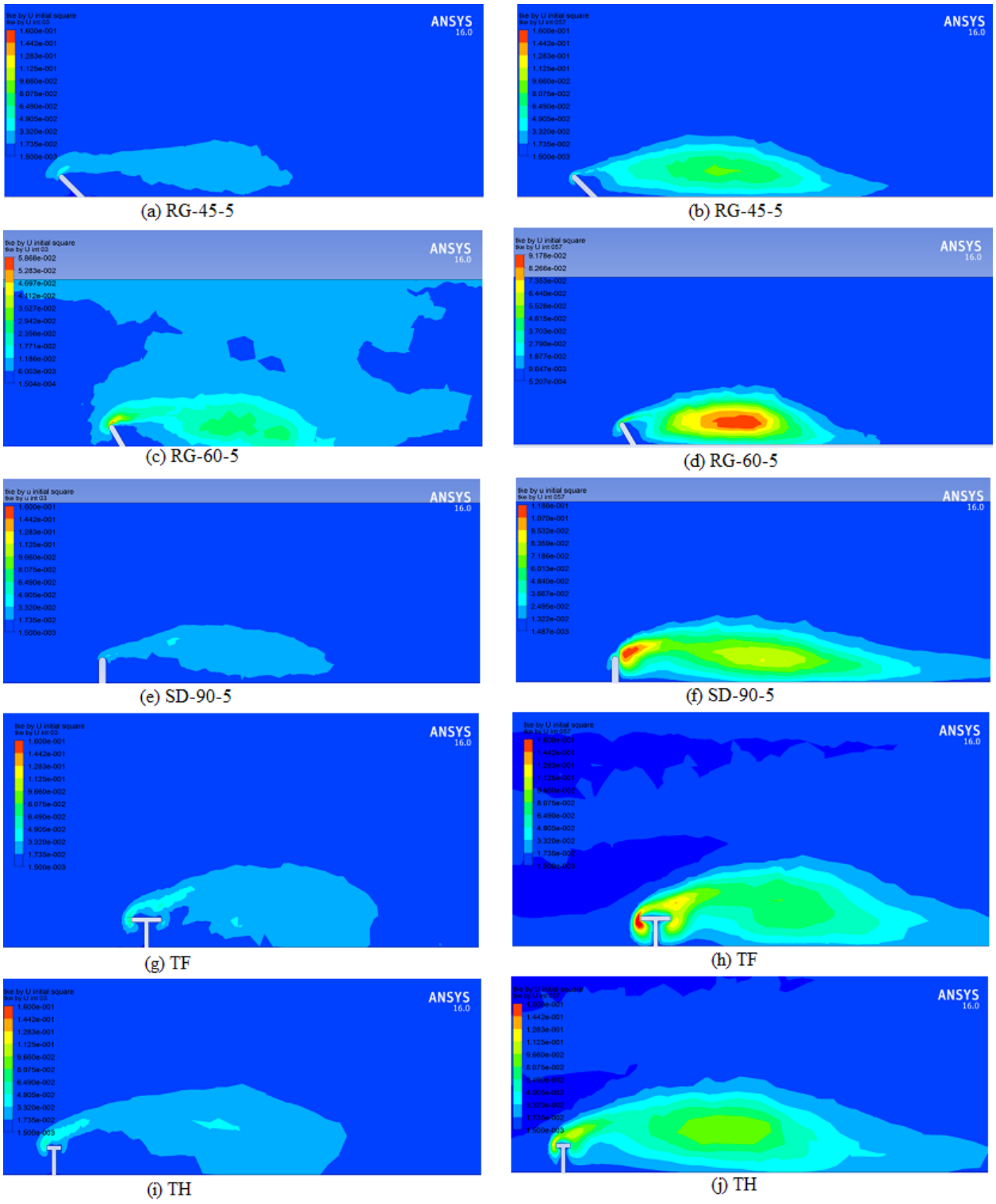

Fig. 4.9. Case 1. Contour of turbulent energy TKE/ U^2_{in} at different horizontal planes for various tested groynes: (a, c, e, g, and i) contour at (Z/H = 0.035) planes; (b, d, f, h, and j) contour at (Z/H = 0.57) planes

Chapter-5

CONCLUSIONS

From the above results and discussion, the following conclusion can be drawn.

1. For repelling & straight SD, regarding the characteristics of the junction flow presented in the literature, approach flow near bed upstream of the groyne separates and a strong HSV forms close to the groyne base. Whereas for TH, HSV is weaker than SD and then HSV completely disappears for TF. Flow complexity in T-shape groyne upstream of it is enhanced by the boundary effects arising from the wing segment.
2. There is negligible effect of Froude Number on protection length or recirculation zone length and width of dynamic shear layer (DSL)
3. Effect of shape of the groyne is more near the bed region than the upper layer around the groyne structure. Two high-velocity zones form at various tested groynes at near bed planes. A velocity amplification zone is concentrated along the outer side of DSL (VA1) and another velocity amplification occurs further away (VA2).
4. Vertical circulation flow is dominant at the upstream part of the TH and distance of HSV core from the bed and also from the groyne structure is longer than SD.
5. TKE decreases rapidly in case of T-shape groyne then others.

Future scope of study

Other special shapes of groyne can also study like L-shape, inverted L-shape, hockey shape of groyne and much more. In the present study we uses the Presto model further study using other models can be done and results from both of models can be obtained and comparison of results using different models can be done.

Chapter- 6

Reference

1. Paik J., and Sotiropoulos F. (2005). “Coherent structure dynamics upstream of a long rectangular block at the side of a large aspect ratio channel.” Phys. Fluids, 17(11), 115104.
2. Kwan T.F. (1988). “A study of abutment scour”. Rep. No. 451, School of Engineering, Univ. of Auckland, Auckland, New Zealand.
3. Kokan M., and Constantinescu G., (2009). “an investigation of dynamics of coherent structures in a turbulent channel flow with a vertical sidewall obstruction.” Phys. Fluids, 21(8), 085104.
4. Ettema R., and Muste M. (2004). “Scale effects in flume experiments on flow around a spur dike in the flat-bed channel.” J. Hydraul. Eng., 10.1061/(ASCE)0733-9429(2004)130:7(635), 635-646.
5. Mukesh Raj Kafle. “Numerical simulations of flow around a spur dike with free surface flow in fixed flat-bed.” journal of the Institute of engineering, vol. 9 No.- 1, pp 107-114.
6. Daniel Hersberger; Mario J. Franca; and Anton J. Schleiss(2015). “wall-roughness effects on flow and scouring in curved channels with gravel beds.” J. Hydraulics Engineering 2016, 14245 04015032, pp 1-10.
7. Francis, J. R. D., A. B. Pattanaik, and S. H. Wearne. "Technical note observations of flow patterns around some simplified groyne structures in channels." ICE Proceedings. Vol. 41. No. 4. Thomas Telford, 1968.
8. Rajaratnam, Nallamuthu, and Benjamin A. Nwachukwu. "Flow near groin-like structures." Journal of Hydraulic Engineering 109.3 (1983): 463-480
9. Ouillon, Sylvain, and Denis Dartus. "Three-dimensional computation of flow around groyne." Journal of hydraulic Engineering 123.11 (1997): 962-970.
10. Mioduszewski, Tomasz, Shiro Maeno, and Yatsugi Uema. "Influence of the spur dike permeability on flow and scouring during a surge pass." International Conference on Estuaries and Coasts. 2003.
11. Ettema, Robert, and Marian Muste. "Scale effects in flume experiments on flow around a spur dike in flat-bed channel." Journal of Hydraulic Engineering (2004).

12. Uijttewaal, Wim S. "Effects of groyne layout on the flow in groyne fields: Laboratory experiments." Journal of Hydraulic Engineering (2005).

13. Yeo, Hong Koo, Joon Gu Kang, and Sung Jung Kim. "An experimental study on tip velocity and downstream recirculation zone of single groynes of permeability change." KSCE Journal of Civil Engineering 9.1 (2005): 29-38.

14. Tang, Xuelin, Xiang Ding, and Zhicong Chen. "Large eddy simulations of three-dimensional flows around a spur dike." Tsinghua Science & Technology 11.1 (2006): 117-123

15. Ho, Yossef, Mohamed FM, and Huib J. de Vriend. "Flow details near river groynes: experimental investigation." Journal of Hydraulic Engineering 137.5 (2010): 504-516

16. McCoy, Andrew, George Constantinescu, and Larry J. Weber. "Numerical investigation of flow hydrodynamics in a channel with a series of groynes."Journal of Hydraulic Engineering 134.2 (2008): 157-172.

17. Duan, Jennifer G. "Mean flow and turbulence around a laboratory spur dike."Journal of Hydraulic Engineering (2009).

18. Safarzadeh, A., et al. "Experimental study of head shape effects on shear stress distribution around a single groyne." River flow 2010, Proceedings of 5th International Conference on Fluvial Hydraulics. 2010.